Nutrition 27 (2011) 488–495

Contents lists available at ScienceDirect

Nutrition

journal homepage: www.nutritionjrnl.com

Basic nutritional investigation

Anti-diabetic effects including diabetic nephropathy of anti-osteoporotic trace minerals on diabetic mice

Fusako Maehira Ph.D. [a,*], Nau Ishimine M.S. [a], Ikuko Miyagi B.S. [a], Yukinori Eguchi Ph.D. [b], Katsumasa Shimada M.D., Ph.D. [c], Daisuke Kawaguchi B.S. [c], Yoshihide Oshiro B.S. [c]

[a] Department of Biometabolic Chemistry, School of Health Sciences, Faculty of Medicine, University of the Ryukyus, Nishihara, Okinawa, Japan
[b] Research Laboratory Center, Faculty of Medicine, University of the Ryukyus, Nishihara, Okinawa, Japan
[c] Department of Morphological Pathology, School of Health Sciences, Faculty of Medicine, University of the Ryukyus, Nishihara, Okinawa, Japan

ARTICLE INFO

Article history:
Received 14 July 2009
Accepted 20 April 2010

Keywords:
Anti-diabetes
Soluble silicon
Stable strontium
Pancreatic and renal gene expression
Diabetic glomerulopathy

ABSTRACT

Objective: In our previous study to evaluate the effects of soluble silicon (Si) on bone metabolism, Si and coral sand (CS) as a natural Si-containing material suppressed peroxisome proliferator-activated receptor γ (PPARγ), which regulates both glucose and bone metabolism and increases adipogenesis at the expense of osteogenesis, leading to bone loss. In this study, we investigated the anti-diabetic effects of bone-seeking elements, Si and stable strontium (Sr), and CS as a natural material containing these elements using obese diabetic KKAy mice.
Methods: Weanling male mice were fed diets containing 1% Ca supplemented with $CaCO_3$ as the control and CS, and diets supplemented with 50 ppm Si or 750 ppm Sr to control diet for 56 d. The mRNA expressions related to energy expenditure in the pancreas and kidney were quantified by real-time polymerase chain reaction.
Results: At the end of feeding, plasma glucose, insulin, leptin, and adiponectin levels decreased significantly in three test groups, while pancreatic PPARγ and adiponectin mRNA expression levels increased significantly toward the normal level, improving the glucose sensitivity of β-cells and inducing a significant decrease in insulin expression. The renal PPARγ, PPARα, and adiponectin expression levels, histologic indices of diabetic glomerulopathy, and plasma indices of renal function were also improved significantly in the test groups.
Conclusion: Taken together, anti-osteoporotic trace minerals, Si and Sr, and CS containing them showed novel anti-diabetic effects of lowering blood glucose level, improving the tolerance to insulin, leptin, and adiponectin, and reducing the risk of glomerulopathy through modulation of related gene expression in the pancreas and kidney.

Introduction

Type 2 diabetes is a systematic disorder characterized by impairment of energy metabolism of macronutrients, carbohydrates, lipids, and proteins, due to insulin resistance. Micronutrients such as vitamins and minerals can regulate metabolism and gene expression and influence the development and progression of diabetes. Among several minerals that have been investigated as potential preventative and treatment agents for diabetes, magnesium, chromium, and vanadium have been reported as agents required for maintenance of normal glucose metabolism in both experimental animals and humans [1].

Soluble silicon (Si) studied in this paper is known as an essential element for the formation of collagen and glycosaminoglycans in bone and cartilage [2,3]. The essentiality of Si and its levels in serum and tissues were reviewed and coral sand (CS) was defined, and its use as a natural Si-containing material was also described in our previous studies [4,5], in which soluble Si and CS induced a significant decrease in the bone marrow expression of proliferator-activated receptor (PPAR) γ of approximately 50%, leading to the stimulation of bone formation. PPARγ, a ligand-activated transcription factor and a member of the nuclear hormone receptor superfamily, is expressed predominantly in adipocytes that share a common pluripotent mesenchymal precursor with osteoblasts [6]. PPARγ plays a critical role in glucose homeostasis and is the molecular target of a class of insulin-sensitizing drugs referred to as thiazolidinediones (TZDs) [7–9], which are widely

* Corresponding author. Tel.: +81 98 895 1277; fax: +81 98 895 1277.
E-mail address: fmaehira@med.u-ryukryu.ac.jp (F. Maehira).

0899-9007/$ - see front matter © 2011 Elsevier Inc. All rights reserved.
doi:10.1016/j.nut.2010.04.007

prescribed for type 2 diabetes. Although the most common adverse effects with TZDs are weight gain and fluid retention, the TZDs appear to have a more durable effect on glycemic control and are currently approved in the U.S. for use in combination with other anti-diabetic drugs [9]. Cumulative evidence indicates that TZDs increase adipogenesis at the expense of osteogenesis, leading to bone loss [10], and a sample of women with diabetes who were randomized with or without TZD treatment demonstrated its association with a high risk of fractures [11,12]. An inverse relationship between adipocytes and osteoblasts has been confirmed in numerous studies [13,14]. In addition, recent studies have addressed a balanced see-saw relationship between fat and bone, in which PPARγ haplo-insufficient mice with a 50% reduction in PPARγ expression due to heterozygous PPARγ deficiency exhibited resistance to high-fat-diet-induced obesity, insulin resistance [15], and also high bone mass with increased osteoblastogenesis [14]. Consistent with these reports, the Pro12Ala polymorphism in human PPARγ2, which moderately reduces the transactivation capacity of PPARγ, is associated with resistance to type 2 diabetes in the general population [16]. On the basis of the available evidence, it is desirable in diabetes to balance an inverse relationship between fat and bone either by developing novel selective PPARγ modulators [17], which have beneficial activities as insulin sensitizers without adverse effects on the skeleton, or by finding bone-seeking minerals exhibiting activities as insulin sensitizers. In this study, we pursue the latter option by examining the anti-diabetic effects of Si, which was found to exhibit a moderate suppressive effect on bone marrow PPARγ [4], stable strontium (Sr), which has been recently shown to have dual effects on bone metabolism, of increasing bone formation and decreasing bone resorption [18], and CS as natural material containing these two minerals, using obese diabetic KKAy mice.

Materials and Methods

Animal experiments

Diabetic 4-wk-old male KKAy/Ta Jcl mice, produced by transfer of the $A^y/+$ gene into the original Japanese KK strain, and normal ICR mice as a reference were purchased from CLEA Japan (Tokyo, Japan). The experimental protocols of this study were approved by the Animal Experiment Ethics Committee of the University of the Ryukyus. KKAy mice were divided into four groups of 10 each and housed one per cage at 24 °C with a 12-h light-dark cycle. Because the primary aim of the study was to evaluate efficacy of anti-osteoporotic minerals in the preventive role in the progression of diabetes, we started to feed KKAy mice at 5 wks old prior to onset glycosuria until 13 wks old after development of diabetes and diabetic nephropathy [19]. Five-wk-old animals were maintained for 56 d on an ad libitum semisolid diet of 34% tap water and 66% powder diet (Table 1) containing 1% Ca supplemented with $CaCO_3$ as the control (CT) and CS in Ca-deficient purified diet (Oriental Yeast, Tokyo, Japan), and diet with 50 ppm Si or 750 ppm Sr added to the CT diet. Doses in the range of 100 to 500 ppm Si have been used in previous studies without toxic effects [2,4,5] and this dose of Sr was one third to one sixth less than the beneficial low dose [18]. An available soluble Si compound, sodium metasilicate, $Na_2SiO_3 \cdot 9H_2O$, and strontium chloride, $SrCl_2 \cdot 6H_2O$, were used in the animal studies. At 0, 15, 37, and 51 d after starting the feeding experiment, tail vein blood glucose levels after 6-h fasting were measured using a Dexter-Z II (Bayer Medical, Tokyo, Japan).

Preparation of samples

At the end of the 56-d experiment, each group of mice was bled to death under anesthesia at regular intervals after 6-h fasting. Heparinized blood was obtained from each mouse by heart puncture under anesthesia and centrifuged, and plasma was divided into aliquots and stored at −80 °C until analysis. The immediately excised pancreas was homogenized using a mini-crusher device for biomaterials, BioMasher (Hi-Tech, Tokyo, Japan): approximately 50 mg tissue was immersed in 500 μL RNAlater reagent (Qiagen, Germantown, MD, USA) into the filter unit in a 1.5 mL centrifuge tube; a crushing stick was inserted as a pestle; then centrifugation at 11 000 × g and 30 s macerated the tissue in the filter unit. The tissue homogenate was quickly frozen in liquid nitrogen. After both kidneys were quickly excised, one kidney was cut longitudinally into two pieces and the kidney tissue was processed by the same method as that used for the pancreatic tissue. The quickly frozen kidney homogenate in liquid nitrogen was stored at −80 °C until the next day for isolation and purification of RNA. Another kidney was fixed in 10% neutral-buffered formalin solution for histologic examination.

Table 1
Mineral composition of 100 g of diet

	Minerals in basal powder		Minerals in the experimental diets			
	Basal diet*	CS	CT	CS	Si	Sr
Ca (g)	0	36.1	1.11	1.11	1.11	1.11
Mg	0.24	2.30	0.23	0.30	0.23	0.23
Na	0.24	0.32	0.23	0.24	0.23	0.23
K	0.87	0.02	0.85	0.84	0.85	0.85
P	0.83	0.00	0.81	0.81	0.81	0.81
Sr (mg)	3.0	280.0	2.9	11.3‡	2.9	75.8‡
Si†	0.02	0.98	0.02	0.05‡	5.02‡	0.02
Fe	32	39	31.1	33.2	31.1	31.1
Zn	5.1	0.47	4.96	4.96	4.96	4.96
Cu	0.75	0.23	0.73	0.73	0.73	0.73
Mn	5.32	17.00	5.17	5.67	5.17	5.17

Ca, calcium; CS, coral sand; CT, calcium carbonate (control); Cu, copper; Fe, iron; K, potassium; Mg, magnesium; Mn, manganese; Na, sodium; P, phosphorus; Si, silicon; Sr, strontium; Zn, zinc

* Ca-deficient basal diet.

† Soluble Si measured by micro-molybdenum blue method [4].

‡ The mineral levels are more than twice that of CT.

Measurements of plasma parameters

Plasma was assayed for glucose, albumin, blood urea nitrogen (BUN), creatinine, triglycerides (TG), and total cholesterol using clinical laboratory kits. Sandwich ELISA kits were used to measure insulin (Mercodia, Uppsala, Sweden), leptin (SPI-BIO, Bretonneux, France), and adiponectin (Phoenix Pharmaceuticals, CA, USA). All samples were measured in duplicate in single batches and averaged. Homeostatic model assessment of insulin resistance (HOMA-IR) was calculated as the fasting plasma insulin (mU/L) × fasting plasma glucose (mmol/L)/22.5 [20].

RNA isolation and gene expression analysis

Immediately after the pancreas was homogenized in each group, total RNA was isolated and purified using a NucleoSpin RNA II kit (Macherey-Nagel GmbH & Co., Düren, Germany) following the manufacturer's protocol. Two micrograms of RNA was used for cDNA synthesis by reverse transcription with an Omniscript RT kit (Qiagen). Quantitative real-time polymerase chain reaction (PCR) was performed using the Mx3000P real-time PCR system (Stratagene, La Jolla, CA, USA) and fluorescent dye SYBR Green (Brilliant SYBR Green QPCR Master Mix, Stratagene) to detect a double-stranded DNA amplicon [4,5]. Gene expression was analyzed using the following pairs of primers: PPARγ, (forward) 5'-CGAGC CCTGGCAAAGCATTTGTAT-3' and (reverse) 5'-TGTCTTTCCTGTCAAGATCGCCCT-3'; PPARα, (forward) 5'-AAGAACCTGAGGAAGCCGTTCTGT-3' and (reverse) 5'-GCA GCCACAAACAGGGAAATGTCA-3'; insulin, (forward) 5'-AAAGGCTCTTTACCTGG TGTGTGG-3' and (reverse) 5'-ACTGATCCACAATGCCACGCTTCT-3'; adiponectin, (forward) 5'-GCACTGGCAAGTTCTACTGCAACA-3' and (reverse) 5'-AGAGAACGG CCTTGTCCTTCTTGA-3'; GAPDH, (forward) 5'-AACGACCCCTTCATTGAC-3' and (reverse) 5'-TCCACCACATACTCAGCAC-3'. All real-time PCR reactions contained first-strand cDNA corresponding to 1–10 ng RNA. The PCR protocol included the following cycling conditions: 95 °C denaturation for 10 min, then 45 cycles of 95 °C denaturation for 30 s followed by 60 °C annealing for 1 min, and 72 °C extension for 30 s. The fluorescent amplicon was primarily detected at the end of the 60 °C annealing period. PCR products were subjected to a melting curve analysis and quantified with Mx3000*P* software v. 1.20c (Stratagene) [4,5]. The sizes of PCR products for mouse PPARγ, PPARα, insulin, adiponectin, and glyceraldehide-3-phosphate dehydrogenase (GAPDH) were 90, 110, 170, 114, and 191 bp, respectively. PCR results were normalized to the expression of GAPDH in the same samples. Triplicate analyses were performed for each sample.

Histologic examinations

Formalin-fixed tissues were embedded in paraffin, cut into 3-μm sections, and mounted on silanized slides. Sections for routine light microscopy were stained with hematoxylin and eosin. For histopathologic examinations of glomerular injury, sections were stained with periodic acid-methenamine-silver stain or the periodic acid-Schiff reagent and 100 glomeruli per mouse were

Table 2
Body weight and average daily intakes of diet, Si, and Sr per mouse

	CT group ($n = 10$)	CS group ($n = 10$)	Si group ($n = 10$)	Sr group ($n = 10$)
Body weight (g) at the end of experiment				
	44.1 ± 1.9	44.8 ± 1.0	43.7 ± 2.7	42.2 ± 1.9
% Increase	154†	162†	155†	155†
% Body weight	100	104	102	104
Average daily intakes (g)				
Diet*	5.89 ± 0.87	6.14 ± 0.61	5.99 ± 0.67	6.14 ± 0.84
% Intake	100	104	102	104
Si (mg)	1.15 ± 0.17	3.0 ± 0.33	300.53 ± 33.47	1.19 ± 0.61
% Intake	100	261‡	26133‡	103
Sr (μg)	0.17 ± 0.03	0.69 ± 0.07	0.17 ± 0.02	4.66 ± 0.63
% Intake	100	406‡	100	2741‡

CS, coral sand; CT, calcium carbonate (control); Si, silicon; Sr, strontium
* Powder diet = solid diet × 0.66.
† $P < 0.001$ versus values at the start of experiment.
‡ $P < 0.001$ versus the CT group.

examined in a blinded manner for mesangial matrix expansion, thickening of Bowman's capsule membrane, and glomerular capillary basal membrane (GCBM). Electronically stored optical microscopic images of glomeruli at ×400 were displayed on a personal computer; average values of scores assessed by a pathologist and two expert technologists were used as the pathologic scores for each mouse. Mesangial matrix expansion was defined as a diffuse accumulation of periodic acid-Schiff positive material in the mesangial area. An arbitrary score to evaluate mesangial matrix expansion was graded from level 0 to 3 as follows: level 0, mesangial matrix of <25% of the glomerular area; levels 1, 2, and 3, mesangial matrix of 25–50%, 50–75%, and >75% of the glomerular area, respectively. Thickening of Bowman's capsule membrane or GCBM was evaluated by counting the presence or absence of the membrane thickening per a glomerulus, as compared with the normal glomerulus displayed in parallel on a computer. The counts from 100 glomeruli were expressed as a percentage per mouse and the score was graded as follows: level 0, the membrane thickening of <10%; levels 1, 2, and 3, the membrane thickening of <25%, 25–50%, and >50% of glomeruli examined, respectively. Finally, the rate of each level for three indices used to assess glomerular injury was expressed as a percentage in each group. The sum of levels 2 and 3 in three test groups was compared with the value of the control group.

Statistical analysis

Experimental results are reported as the mean ± SD of the average of triplicate independent samples for quantitative real-time PCR analysis and of duplicate analyses for animal specimens, unless otherwise indicated. Statistical analyses were performed by comparing mean values using either one-way analysis of variance with the SAS program (SAS Institute, Cary, NC, USA) or Student's two-tailed t test as appropriate. Individual differences between groups were assessed using Duncan's multiple range test, in which means with different letters are significantly different at a P value of less than 0.05.

Results

Effects on blood and plasma parameters

All animals appeared healthy during the study period and there were no significant differences in diet intake and weight gain among groups at the end of the experiment. The average daily intake of minerals per mouse adjusted for the average dietary intake through the experimental period is presented in Table 2. Increased Si intake was determined to be 261-fold in the Si group and 2.6-fold in the CS group and Sr intake as 27-fold in the Sr group and 4-fold in the CS group compared with the CT group, because of its rapid elimination from the circulation into urine, as described in the last part of the discussion. Tail vein blood glucose in three test groups after 37 d remained significantly low at 70% of the control value (Fig. 1). Comparing the CT plasma values at the end of the 8-wk experiment, glucose (76% in CS, 84% in Si, 55% in Sr, and 34% in ICR normal mice), insulin (54%, 68%, 73%, and 16%), HOMA-IR (42%, 59%, 40%, and 5%), adiponectin (63%, 70%, 45%, and 51%), and leptin (75%, 76%, 71%, and 20%) were suppressed significantly to low values close to the normal levels in the test groups (Fig. 2), preventing the progression to the resistance of insulin, adiponectin, and leptin observed in diabetic control mice. Plasma indices related to kidney function also remained at the values close upon the normal level in the test groups compared to the diabetic control mice, as seen in the elevated albumin and reduced BUN, creatinine, and TG levels (Table 3).

Effects on gene expression of pancreas and kidney

Compared with those in the CT pancreas, the mRNA expression of PPARγ (117% in CS, 135% in Si, 181% in Sr, and 164% in ICR normal mice) and adiponectin (128%, 127%, 117%, and 145%) increased significantly toward the normal level, improving the glucose sensitivity of β-cells and decreasing the insulin expression (21%, 9%, 55%, and 11%), as presented in Figure 3. In addition, the renal expression of PPARγ (133% in CS, 141% in Si, and 136% in Sr), adiponectin (153%, 135%, and 123%), and PPARα (161%, 171%, and 169%) increased significantly in the three test groups (Fig. 4),

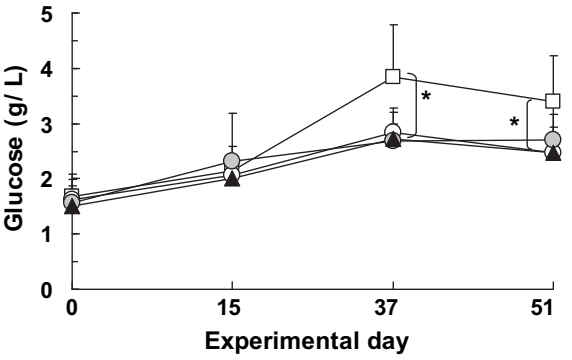

Fig. 1. Effects on tail venous glucose in mice fed diets containing 1% Ca supplemented with $CaCO_3$ as the control (CT, white square), coral sand (CS, white circle) in Ca-deficient purified diet, and 50 ppm Si (Si, grey circle) or 750 ppm Sr (Sr, black triangle) supplementation to the CT diet, as described in Materials and Methods. Values are means ± standard deviations for 10 animals in each group. $*P < 0.05$ versus the control group.

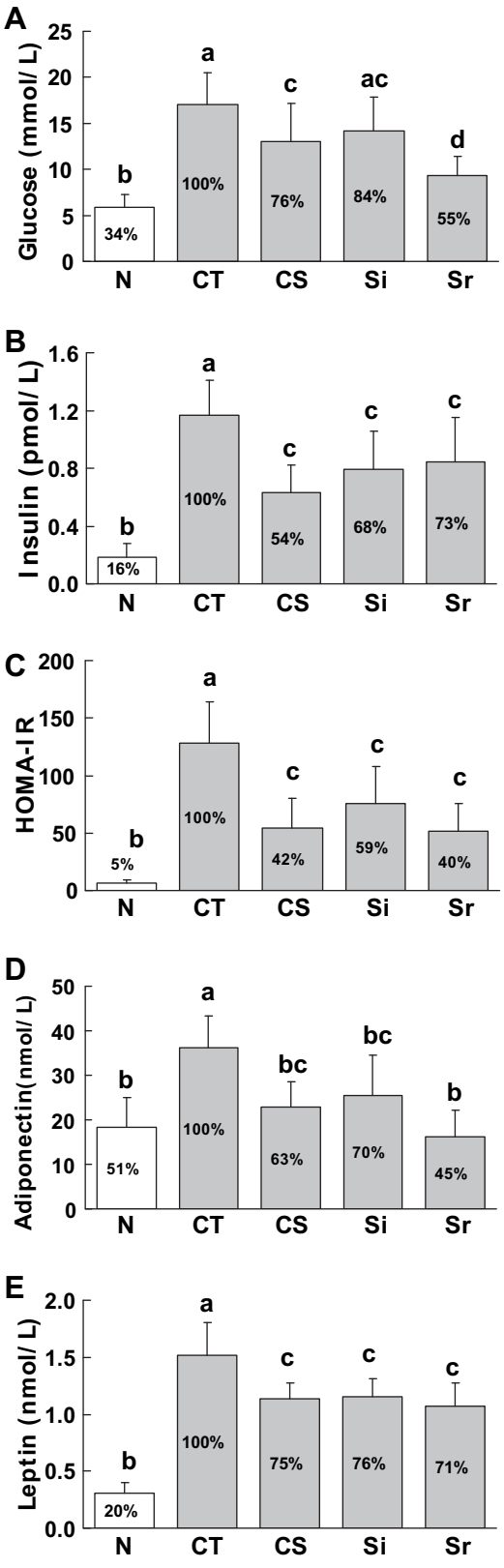

Fig. 2. Effects on plasma levels of glucose (A), insulin (B), HOMA-IR (C), adiponectin (D), and leptin (E). Values are means ± standard deviations. Means with different letters are significantly different at $P < 0.05$ (Duncan's new multiple range test). CS, coral sand; CT, calcium carbonate (control); N, normal ICR mice; Si, silicon; Sr, strontium.

suggesting a protective effect from diabetic nephropathy by ameliorating lipid homeostasis.

Histologic examination of renal glomerular injury

Compared with that for CT, histopathologic examination by grading the severity of glomerular injury showed a marked reduction in mesangial matrix expansion, thickening of Bowman's capsule membrane, and GCBM in the three test groups (Fig. 5).

Discussion

An adipose-derived hormone, leptin, suppresses the activity of neuropeptide Y/agouti-related protein neurons that stimulate food intake [21]. Relative or absolute insensitivity to leptin at its site of action induces the increased circulating leptin levels in obese rodents and humans [21]. The mouse model of obesity-associated type 2 diabetes used in the present study, KKAy mice overexpressing agouti-related protein, is characterized by hyperleptinemia, hyperinsulinemia, and hyperlipidemia [21], as shown in Figure 2 and Table 3. Hyperinsulinemia may be derived from reduced suppression of proinsulin gene expression and insulin secretion by leptin resistance in pancreatic β-cells [22]. Insulin resistance in KKAy control mice was confirmed by 20-fold HOMA-IR compared with that of normal mice (Fig. 2C), which is used to obtain an estimate of insulin resistance and β-cell function [20]. In addition to the resistance to insulin and leptin, adiponectin resistance shown as hyperadiponectinemia was observed in control KKAy mice (Fig. 2D). Adiponectin, adipose-derived hormone, acts as an antidiabetic adipocytokine through an insulin-sensitizing effect mediated by an increase in fatty acid oxidation and glucose uptake via activation of 5'-AMP-activated protein kinase (AMPK) and PPARα [23,24]. The observed hyperadiponectinemia in the diabetic control KKAy mice can be explained by a recent study [25] in which insulin negatively regulated the expression levels of adiponectin receptors and adiponectin sensitivity via the insulin/phosphoinositide 3-kinase/Fox 1 pathway; therefore, obesity-linked insulin resistance/hyperinsulinemia can down-regulate adiponectin receptors and thus adiponectin resistance. Plasma indices observed in the diabetic control KKAy mice such as hyperglycemia, resistance to insulin, adiponectin, and leptin (Fig. 2), and hypertriglyceridemia (Table 3), remained the values close to normal levels in the three test groups at the end of the 8-wk experiment. An attempt to elucidate a possible mechanism behind the observed improvements caused by bone-seeking elements, Si and Sr, and CS, was made by analyses of the mRNA expressions in the pancreas and kidney (Figs. 3 and 4) together with the cumulative evidence from previous studies.

In the pancreas of KKAy mice in this study, overexpression of insulin mRNA with an approximately 10-fold increase over normal ICR mice (Fig. 3B) may have originated from a compensatory response to hyperglycemia (Figs. 1 and 2A) and increased insulin secretion due to leptin resistance at the level of the pancreatic β-cells [22]. The resulting hyperinsulinemia (Fig. 2B) promotes both insulin resistance and leptin production by adipose tissue (Fig. 2E), which may in turn enhance leptin resistance of pancreatic β-cells with subsequent establishment of adipoinsular axis dysregulation and lead to the diabetic state in obese animals and subjects [22]. In addition, reduced adiponectin sensitivity as indicated by hyperadiponectinemia (Fig. 2D) due to decreased expression of adiponectin receptors induced by hyperinsulinemia [25] may also decrease the energy expenditure

Table 3
Plasma indices related to kidney function

	Albumin		BUN		Creatinine		Triglycerides		T-CHO	
	(g/L)	(%)	(mg/L)	(%)	(mg/L)	(%)	(mg/L)	(%)	(mg/L)	(%)
N group	27.9 ± 1.0†	120	318 ± 47†	69	1.2 ± 0.3*	44	401 ± 63†	31	1203 ± 96	111
CT group	23.3 ± 2.3	100	459 ± 78	100	2.7 ± 1.2	100	1280 ± 140	100	1085 ± 36	100
CS group	26.0 ± 1.5*	112	415 ± 64	90	2.0 ± 1.2	74	755 ± 149†	59	988 ± 108	91
Si group	26.0 ± 2.1*	112	410 ± 43	89	1.3 ± 1.0*	48	560 ± 89†	44	1208 ± 125	111
Sr group	27.0 ± 3.3*	116	369 ± 56*	80	2.0 ± 1.4	74	533 ± 94†	42	1110 ± 91	102

BUN, blood urea nitrogen; CS, coral sand; CT, calcium carbonate (control); N, normal ICR mice; Si, silicon; Sr, strontium; T-CHO, total cholesterol
Data are presented as means ± SD.
Basal data provided by CLEA Japan (Tokyo, Japan) for KKAy/Ta Jcl (CT) and ICR (N) at 10-wk-old and $n = 10$ each:
Albumin, (CT) 29.7 ± 1.9 versus (N) 33.1 ± 1.5*; BUN, (CT) 314 ± 19 versus (N) 285 ± 35†; Creatinine (CT) 3.8 ± 0.2 versus (N) 1.0 ± 0.2†; Triglycerides (CT) 1576 ± 422 versus (N) 480 ± 129†. Glycosuria for CT, (10-wk-old) 100% positive versus (5-wk-old) 100% negative. Proteinurea for CT, (10-wk-old) 100% positive with 300–1000 mg/L versus (5-wk-old) 90% positive with 100–300 mg/L. Values at 10-wk-old are similar to those at 18-wk-old .
* $P < 0.05$
† $P < 0.001$ versus the CT group.

in muscle and adipose tissue of diabetic mice. Such vicious cycle may have been improved by significant increases in the mRNA expression of PPARγ in pancreatic β-cells of the three test groups compared with that of the control group (Fig. 3A). Activation of PPARγ restored leptin resistance/hyperleptinemia in the three test groups (Fig. 2E) through its inhibitory regulation of leptin expression [26], with a subsequent improvement of insulin expression [21] (Fig 3B) followed by the systemic recovery of adiponectin sensitivity (Fig. 2D) through release from suppressed expression of adiponectin receptors by insulin [25]. The significant decreases in plasma TG concentrations observed in the three test groups compared with the control group (Table 3) also contributed to improving insulin resistance since fatty acid (FA), whose intracellular concentration tends to run parallel to that of plasma TG, is involved in both insulin resistance and β-cell failure, which is referred to as lipotoxicity [27].

Loss of glucose-stimulated insulin secretion, which is a characteristic feature of obesity-associated type 2 diabetes, is derived from the loss of glucose-sensing ability, which involves glucose transporter isotype 2 (GLUT2) coupled with glucokinase (GK) [28]. Rate-limiting regulators of glucose uptake and its oxidation in pancreatic β-cells, GLUT2 and GK, are directly activated by PPARγ [29] and the mRNA expression of GLUT2 and GK are reduced in diabetic β-cells [30]. In addition to systemic insulin-sensitizing effects of PPARγ activation, its recovery of activation to the normal level in pancreas observed in three test groups (Fig. 3A) may restore the glucose-sensing ability of β-cells, and thus glucose uptake and its oxidation of pancreatic β-cells by stimulating the mRNA expression of GLUT2, GK as reported by Kim and Ahn [29]. A PPARγ agonist, troglitazone, is also reported to stimulate glucose-stimulated insulin secretion directly from pancreatic β-cells [31], thus improving insulin

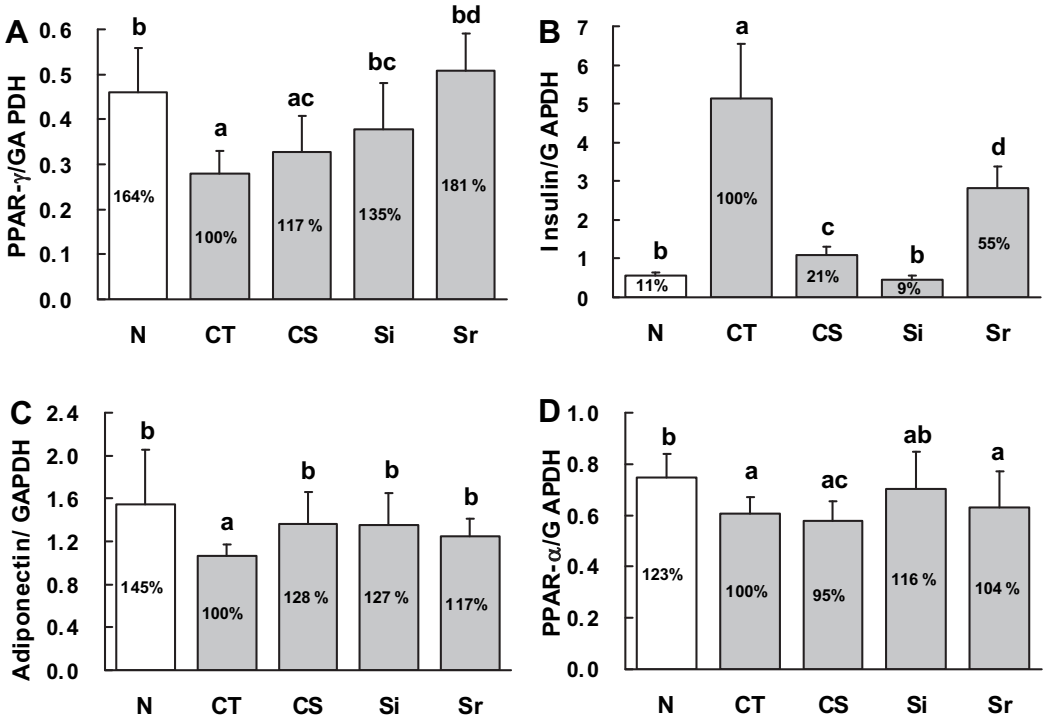

Fig. 3. Effects on gene expression of pancreas. (A) PPARγ, (B) insulin (×10 000), (C) adiponectin, and (D) PPARα. Values are means ± standard deviations. Means with different letters are significantly different at $P < 0.05$. CS, coral sand; CT, calcium carbonate (control); GAPDH, glyceraldehyde-3-phosphate dehydrogenase; N, normal ICR mice; PPARγ, peroxisome proliferator-activated receptor γ; PPARα, peroxisome proliferator-activated receptor α; Si, silicon; Sr, strontium.

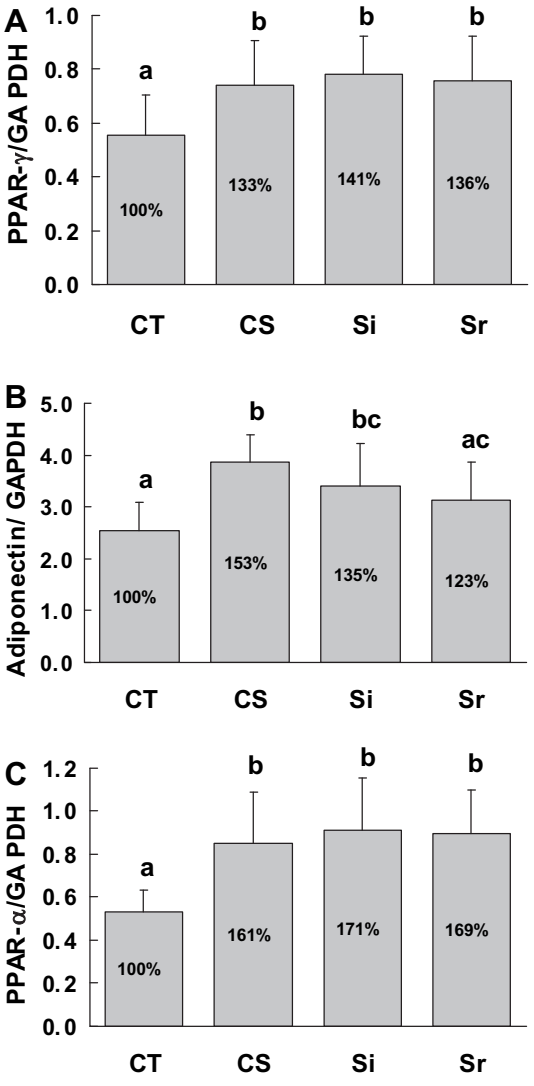

Fig. 4. Effects on gene expressions of kidney. (A) PPARγ, (B) adiponectin (×1000), and (C) PPARα. Values are means ± standard deviations. Means with a different letter are significantly different at $P < 0.05$. CS, coral sand; CT, calcium carbonate (control); GAPDH, glyceraldehide-3-phosphate dehydrogenase; PPARγ, peroxisome proliferator activated receptor γ; PPARα, peroxisome proliferator activated receptor α; Si, silicon; Sr, strontium.

resistance. Moreover, PPARγ promotes the gene expression of both adiponectin [32] (Fig. 3C) and its receptors [33,34], which also improves insulin resistance in pancreatic β-cells by increasing glucose uptake and its oxidation as well as FA oxidation via AMPK activation [35]. Another isotype of nuclear receptors, PPARα, regulates the expression of various genes related to lipid metabolism, including genes involved in uptake, binding, and oxidation of FA [36]. Beta-cell function may improve with dual PPARα/γ [37] or pan-PPAR [38] agonist therapy, as both PPARα and -γ are expressed in β-cells. The pancreatic PPARα expression of all KKAy mice groups (Fig 3D) was however slightly suppressed to 81% in CT, 77% in CS, 94% in Si, and 86% in Sr, respectively, compared with normal ICR mice, while plasma glucose concentrations in KKAy mouse groups ranged from 9 to 17 mmol/L (Fig. 2A). The results are consistent with a study [39] in which chronic exposure of β-cells to a supraphysiologic glucose level led to a 60–80% reduction in PPARα mRNA expression.

Diabetic nephropathy (DN) has now become the leading cause of chronic and end-stage renal disease and is characterized by albuminuria, hypertension, and reduced renal function [40]. Hyperglycemia is a primary risk factor for the initiation and progression of renal microvascular injury, and dyslipidemia also contributes to kidney injury [41]. Proteinuria is a marker of disease severity and is considered to play a central role in the pathogenesis of progressive renal dysfunction. Nephropathy was classified as absent, microalbuminuria, or persistent proteinuria. "Absent" was defined as albumin-to-creatinine ratio (ACR) in spot urine <30 mg/gCr; microalbuminuria was defined as 30 mg/gCr ≤ACR <300 mg/gCr; proteinuria was defined as ACR ≥300 mg/gCr. In the studies about patients with type 2 diabetic mellitus [42,43], the results of regression analyses with adjustment for the variables revealed that serum albumin was independently and inversely related to the severity of proteinuria. As presented in Table 3, the plasma albumin level measured in this study and both plasma creatinine and TG concentrations were markedly improved in the three test groups toward the normal level together with a reduction in plasma glucose (Figs. 1 and 2A), indicating preventive effects on factors promoting progression of DN. Since cumulative evidence indicates the participation of insulin resistance in the pathogenesis of DN in type 2 diabetes, insulin sensitizers, both PPARγ [44] and PPARα [45] agonists, exert protective effects on DN. Moreover, the combination of PPARα and PPARγ agonists exhibited additive and synergistic effects on complications in DN [46]. Our renal gene expression study results showed significant increases of both PPARγ and PPARα mRNA expression together with adiponectin mRNA expression in the three test groups compared with control KKAy mice (Fig. 4), which were associated with improved glomerular function, as presented in Table 3. Since the importance of glomerular injury, including increased thickness of the GCBM, augmentation of glomerular extracellular matrix, and mesangial expansion, is recognized as a pathologic signature of DN [40], we examined the effects of bone-seeking elements, Si, Sr, and CS, on histologic abnormalities in diabetic glomerulopathy. In an early study of KKAy mice [19], the early onset and rapid development of GCBM thickness were evident by 3 mo of age in the KKAy mice in comparison with the non-diabetic normal mice and other diabetic animal models. As presented in Figure 5, a marked improvement in mesangial matrix expansion, thickening of Bowman's capsule membrane, and GCBM was observed in the three test groups at 13 wks old, exhibiting protective effects on DN progression.

Overall, among the three test groups, the Sr group exhibited the most efficient improvement of plasma indices of glucose, adiponectin (Fig. 2A and D), albumin, TG, BUN, creatinine (Table 3), pancreatic PPARγ mRNA expression (Fig. 3A), and histologic glomerulopathy indices (Fig. 5), followed by the Si group. The observed differences between the two minerals may be derived from their distinct pharmacokinetic behaviors. The half-life of the urinary Sr:creatinine ratio and cumulative urinary excretion over days 0–6 were 40 h and 16% of the ingested dose, respectively, and the renal clearance of Sr was less than 4 mL/min, indicating tubular reabsorption of Sr [47]. On the other hand, Si in serum and tissues is present almost entirely as free soluble monosilicic acid, which freely diffuses across the cellular membrane, resulting in its rapid renal clearance: on average, 50% of the ingested Si dose was absorbed and eliminated in urine within 48 h with half-lives of 2.7 h and 11.3 h for 90% and 10%, respectively, and the latter slower component may represent an intracellular fraction with a physiological function [48,49]. The

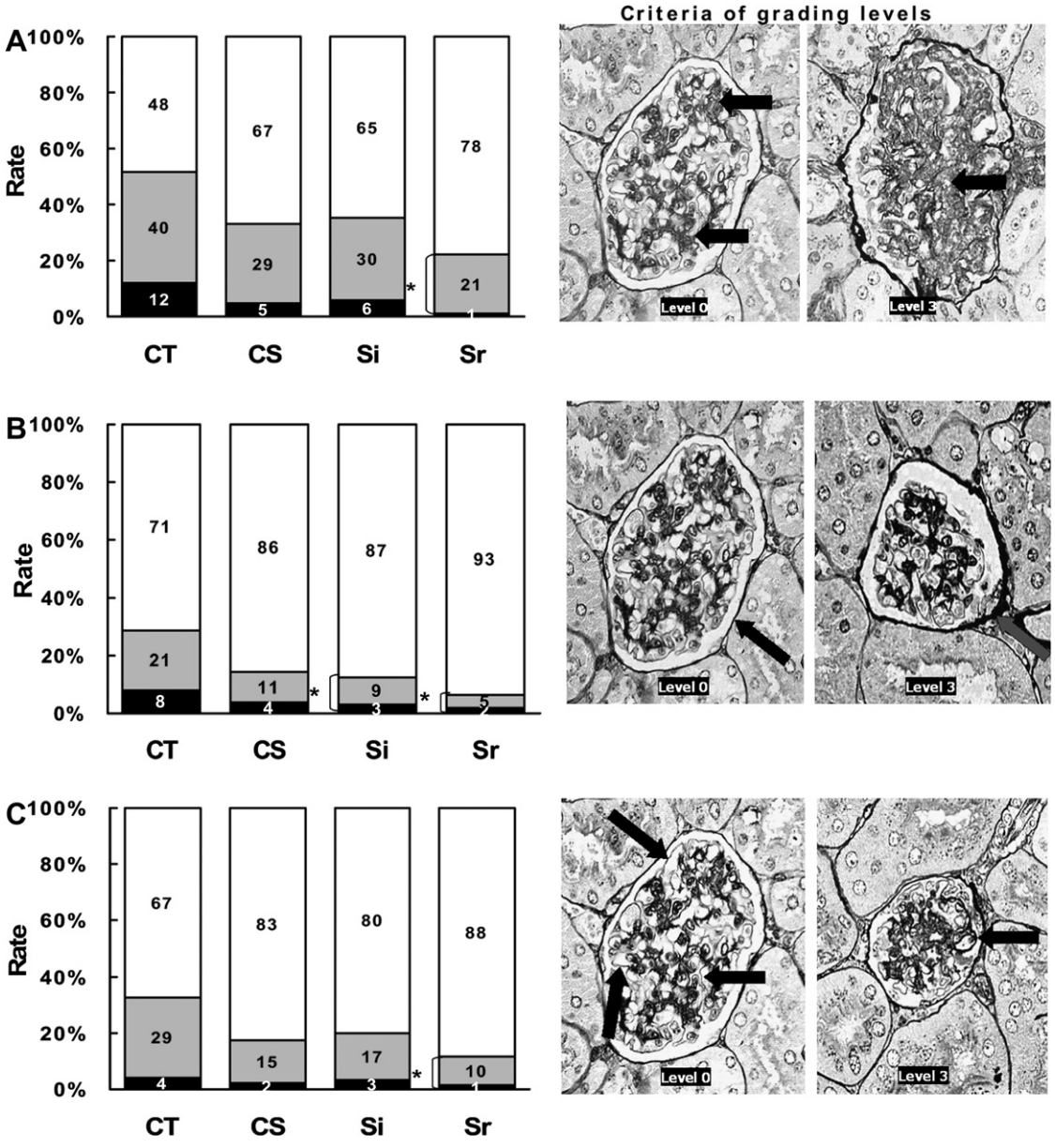

Fig. 5. Histologic examination (periodic acid-methenamine-silver staining, ×400) by grading the severity of glomerular injury showed a marked reduction in mesangial matrix expansion (A), Bowman's capsule membrane thickening (B), and the glomerular capillary basal membrane thickening (C) in the three test groups. The sum of levels 2 and 3 is summarized in the graph and compared with the value of the control group. $*P < 0.05$ versus the control group. Criteria of grading levels (levels 0 and 1, white bars; level 2, gray bars; level 3, black bars) are described in Materials and Methods. CS, coral sand; CT, calcium carbonate (control); Si, silicon; Sr, strontium.

renal clearance of Si was 82–96 mL/min, suggesting high renal filterability and a low tubular reabsorption of Si. Such rapid clearance of inorganic Si may be a potential benefit of long-term intake without excessive retention and accumulation in the body. This study also suggests not only the role of anti-osteoporotic trace minerals in the prevention of progression to diabetes, but the prevention of fracture, one of the complications of diabetes [10–12]. Research including long-term trials is needed to assess the safety and potentially beneficial roles of Si, Sr, and CS as natural material containing two elements in the prevention and management of type 2 diabetes.

In conclusion, this study shows, to our knowledge, a novel function of anti-osteoporotic trace minerals, Si and Sr, and CS containing them, namely, anti-diabetic effects of lowering blood glucose, improving the tolerance to insulin, leptin, and adiponectin, and reducing the risk of glomerulopathy by modulating the expression of related genes in the pancreas and kidney.

References

[1] O'Connell BS. Select vitamins and minerals in the management of diabetes. Diabetes Spectrum 2001;14:133–48.
[2] Carlisle EM. Silicon: an essential element for the chick. Science 1972;178:619–21.
[3] Carlisle EM. Silicon. In: Frieden E, editor. Biochemistry of the essential ultratrace elements. New York: Plenum Press; 1984. p. 257–91.
[4] Maehira F, Miyagi I, Eguchi Y. Effects of calcium sources and soluble silicate on bone metabolism and the related gene expression in mice. Nutrition 2009;25:581–9.
[5] Maehira F, Iinuma Y, Eguchi Y, Miyagi I, Teruya S. Effects of soluble silicon compound and deep-sea water on biochemical and mechanical properties of bone and the related gene expression in mice. J Bone Miner Metab 2008;26:446–55.

[6] Pittenger MF, Mackay AM, Beck SC, Jaiswal RK, Douglas R, Mosca JD, et al. Multilineage potential of adult human mesenchymal stem cells. Science 1999;284:143–7.
[7] Yki-Jarvinen H. Thiazolidinediones. N Engl J Med 2004;351:1106–18.
[8] Kahn SE, Zinman B. Point: Recent long-term clinical studies support an enhanced role for thiazolidinediones in the management of type 2 diabetes. Diabetes Care 2007;30:1672–6.
[9] Nathan DM, Buse JB, Davidson MB, Ferrannini E, Holman RR, Sherwin R, et al. Medical management of hyperglycemia in type 2 diabetes: a consensus algorithm for the initiation and adjustment of therapy—a consensus statement of the American Diabetes Association and the European Association for the Study of Diabetes. Diabetes Care 2009;32:193–203.
[10] Lazarenko OP, Rzonca SO, Hogue WR, Swain FL, Suva LJ, Lecka-Czernick B. Rosiglitazone induces decreases in bone mass and strength that are reminiscent of aged bone. Endocrinology 2007;148:2669–80.
[11] Schwarz AV, Sellmeyer DE, Vittinghoff E, Palermo L, Lecka-Czernick B, Feingold KR, et al. Thiazolidinedione use and bone loss in older diabetic adults. J Clin Endoclinol Metab 2006;91:3349–54.
[12] Kahn SE, Zinman B, Lachin JM, Haffner SM, Herman WH, Holman RR, et al. Rosiglitazone-associated fractures in type 2 diabetes. An analysis from a diabetes outcome progression trial (ADOPT). Diabetes Care 2008;31:845–51.
[13] Lecka-Czernick B, Gubrij I, Moerman EJ, Kajkenova O, Lipschitz DA, Manolagas SC, et al. Inhibition of OSF2/Cbfa1 expression and terminal osteoblast differentiation by PPARγ2. J Cell Biochem 1999;74:357–71.
[14] Akune T, Ohba S, Kamekura S, Yamaguchi M, Chung U, Kubota N, et al. PPARγ insufficiency enhances osteogenesis through osteoblast formation from bone marrow progenitors. J Clin Invest 2004;113:846–55.
[15] Yamauchi T, Kamon J, Waki H, Murakami K, Motojima K, Komeda K, et al. The mechanism by which both heterozygous peroxisome proliferator-activated receptor γ (PPARγ) deficiency and PPARγ agonist improve insulin resistance. J Biol Chem 2001;276:41245–54.
[16] Scacchi R, Pinto A, Rickards O, Pacella A, De Stefano GF, Cannella C, et al. An analysis of peroxisome proliferator-activated receptor gamma (PPAR-γ2) Pro12Ala polymorphism distribution and prevalence of type 2 diabetes mellitus (T2DM) in world populations in relation to dietary habits. Nutr Metab Cardiovasc Dis 2007;17:632–41.
[17] Lazarenko OP, Rzonca SO, Suva LJ, Lecka-Czernick B. Netoglitazone is a PPAR-gamma ligand with selective effects on bone and fat. Bone 2006;38:74–84.
[18] Dahl SG, Allain P, Marie PJ, Mauras Y, Boivin G, Ammann P, et al. Incorporation and distribution of strontium in bone. Bone 2001;28:446–53.
[19] Diani AR, Sawada GA, Zhang NY, Wyse BM, Connell CL, Vidmar TJ, et al. The KKAy mouse: a model for the rapid development of glomerular capillary basement membrane thickening. Blood Vessels 1987;24:297–303.
[20] Matthews DR, Hosker JP, Rundenski AS, Naylor BA, Treacher DF, Turner RC. Homeostasis model assessment: insulin resistance and β–cell function from fasting plasma glucose and insulin concentrations in man. Diabetologia 1985;28:412–9.
[21] Friedman JM, Halaas JL. Leptin and the regulation of body weight in mammals. Nature 1998;395:763–70.
[22] Keiffer TJ, Habener JF. The adipoinsular axis: effects of leptin on pancreatic beta-cells. Am J Physiol Endocrinol Metab 2000;278:E1–14.
[23] Yamauchi T, Kamon J, Minokoshi Y, Ito Y, Waki H, Uchida S, et al. Adiponectin stimulates glucose utilization and fatty-acid oxidation by activating AMP-activated protein kinase. Nat Med 2002;8:1288–95.
[24] Yoon MJ, Lee GY, Chung J-J, Ahn YH, Hong SH, Kim JB. Adiponectin increases fatty acid oxidation in skeletal muscle cells by sequential activation of AMP-activated protein kinase, p38 mitogen-activated protein kinase, and peroxisome proliferator-activated receptor-α. Diabetes 2006;55:2562–70.
[25] Tsuchida A, Yamauchi T, Ito Y, Hada Y, Maki T, Takekawa S, et al. Insulin/Fox 1 pathway regulates expression levels of adiponection receptors and adiponectin sensitivity. J Biol Chem 2003;279:30817–22.
[26] Hollenberg AN, Susulic VS, Madura JP, Zhang B, Moller DE, Tontonoz P, et al. Functional antagonism between CCAAT/enhancer binding protein-α and peroxisome proliferator-activated receptor-γ on the leptin promoter. J Biol Chem 1997;272:5283–90.
[27] McGarry JD, Dobbins RL. Fatty acids, lipotoxicity and insulin secretion. Diabetologia 1999;42:128–38.
[28] Schuit FC, Huypens P, Heimberg H, Pipeleers DG. Glucose sensing in pancreatic beta-cells: a model for the study of other glucose-regulated cells in gut, pancreas, and hypothalamus. Diabetes 2001;50:1–11.
[29] Kim HI, Ahn YH. Role of peroxisome proliferator-activated receptor-γ in the glucose-sensing apparatus of liver and β-cells. Diabetes 2004;53:S60–5.
[30] Del Guerra S, Lupi R, Marselli L, Masini M, Bugliani M, Sbrana S, et al. Functional and molecular defects of pancreatic inslets in human type 2 diabetes. Diabetes 2005;54:727–35.
[31] Kawai T, Hirose H, Seto Y, Fujita H, Fujita H, Ukeda K, et al. Troglitazone ameliolates lipotoxicity in the beta cell line INS-1 expressing PPAR gamma. Diabetes Res Clin Pract 2002;56:83–92.
[32] Maeda N, Takahashi M, Funahashi T, Kihara S, Nishizawa H, Kishida K, et al. PPARγ ligands increase expression and plasma concentrations of adiponection, and adipose-derived protein. Diabetes 2001;50:2094–9.
[33] Kharroubi I, Rasschaert J, Eizirik DL, Cnop M. Expression of adiponectin receptors in pancreatic β cells. Biochem Biophys Res Commun 2003;312:1118–22.
[34] Sun X, Han R, Wang Z, Chen Y. Regulation of adiponectin receptors in hepatocytes by the peroxisome proliferator-activated receptor-γ agonist rosiglitazone. Diabetologia 2006;49:1303–10.
[35] Huypens P, Moens K, Heimberg H, Ling Z, Pipeleers D, Van de Casteele M. Adiponectin-mediated stimulation of AMP-activated protein kinase (AMPK) in pancreatic beta cells. Life Sci 2005;77:1273–82.
[36] Zhou YT, Shimabukuro M, Wang MY, Lee Y, Higa M, Milburn JL, et al. Role of peroxisome proliferator-activated receptor alpha in disease of pancreatic beta cells. Proc Natl Acad Sci USA 1998;95:8898–903.
[37] Kendall DM, Rubin CJ, Mohideen P, Ledeine J-M, Belder R, Gross J, et al. Improvement of glycemic control, triglycerides, and HDL cholesterol levels with Muraglitazar, a dual (α/γ) peroxisome proliferator–activated receptor activator, in patients with type 2 diabetes inadequately controlled with metformin monotherapy. A double-blind, randomized, pioglitazone-comparative study. Diabetes Care 2006;29:1016–23.
[38] Fernandes-Santos C, Carneiro RE, Mendonca LS, Aguila MB, Mandarim-de-Lacerda CA. Pan-PPAR agonist beneficial effects in overweight mice fed a high-fat high-sucrose diet. Nutrition 2009;25:818–27.
[39] Roduit R, Morin J, Masse F, Segall L, Roche E, Newgard CB, et al. Glucose down-regulates the expression of the peroxisome proliferator-activated receptor-α gene in the pancreatic β-cell. J Biol Chem 2000;275:35799–806.
[40] Jefferson JA, Shankland SJ, Pichler RH. Proteinuria in diabetic kidney disease: a mechanistic viewpoint. Kidney Int 2008;74:22–36.
[41] Kaene WF. The role of lipids in renal disease: future challenges. Kidney Int 2000;75:S27–31.
[42] Iwasaki T, Togashi Y, Terauchi Y. Significant association of serum albumin with severity of retinopathy and neuropathy, in addition to that of nephropathy, in Japanese type 2 diabetic patients. Endocr J 2008;55: 311–6.
[43] Leehey DJ, Kramer HJ, Daoud TM, Chatha MP, Isreb MA. Progression of kidney disease in type 2 diabetes—beyond blood pressure control: an observational study. BMC Nephrol 2005;6:8.
[44] Buckingham RE, Al-Barazanji KA, Toseland CDN, Slaughter M, Connor SC, West A, et al. Peroxisome proliferator-activated receptor-γ agonist, rosiglitazone, protects against nephropathy and pancreatic islet abnormalities in Zucker fatty rats. Diabetes 1998;47:1326–34.
[45] Park CW, Zhang Y, Zhang X, Wu J, Chen L, Cha DR, et al. PPAR-α agonist fenofibrate improves diabetic nephropathy in db/db mice. Kidney Int 2006;69:1511–7.
[46] Cha DR, Zhang X, Zhang Y, Wu J, Su D, Han JY, et al. PPAR-α/γ agonist Tesaglitazar attenuates diabetic nephropathy in db/db mice. Diabetes 2007;56:2036–45.
[47] Leeuwenkamp OR, van der Vijgh WJF, Husken BCP, Lips P, Netelenbos JC. Human pharmacokinetics of orally administered strontium. Calcif Tissue Int 1990;47:136–41.
[48] Poppwell JF, King SJ, Day JP, Ackrill P, Fifield LK, Cresswell RG, et al. Kinetics of uptake and elimination of silicic acid by a human subject: a novel application of ^{32}Si and accelerator mass spectorometry. J Inorg Biochem 1998;69:177–80.
[49] Reffitt DM, Jugdaohsingh R, Thompson RPH, Powell JJ. Silicic acid: its gastrointestinal uptake and urinary excretion in man and effects on aluminium excretion. J Inorg Biochem 1999;76:141–7.